Bisecting Microfluidic Channels with Metallic Nanowires Fabricated by Nanoskiving

Kalkman, Gerard A; Zhang, Yanxi; Monachino, Enrico; Mathwig, Klaus; Kamminga, Machteld; Pourhossein Aghbolagh, Parisa; Oomen, Pieter E; Stratmann, Sarah A; Zhao, Zhiyuan; van Oijen, Antonius

Published in:
Acs Nano

DOI:
10.1021/acsnano.5b07996

Publication date:
2016

Bisecting Microfluidic Channels with Metallic Nanowires Fabricated by Nanoskiving

Gerard A. Kalkman,[†,‡] Yanxi Zhang,[†,¶,§] Enrico Monachino,[†,¶] Klaus Mathwig,[‡] Machteld E. Kamminga,[¶] Parisa Pourhossein,[¶,§] Pieter E. Oomen,[‡] Sarah A. Stratmann,[¶] Zhiyuan Zhao,[¶,§] Antoine M. van Oijen,[*,¶] Elisabeth Verpoorte,[*,‡] and Ryan C. Chiechi[*,¶,§]

†*These authors contributed equally to this work.*

‡*Groningen Research Institute of Pharmancy, Antonius Deusinglaan 1, 9713 AV Groningen The Netherlands.*

¶*Zernike Institute for Advanced Materials, Nijenborgh 4, 9747 AG Groningen, The Netherlands*

§*Stratingh Institute for Chemistry, University of Groningen, Nijenborgh 4, 9747 AG Groningen, The Netherlands*

E-mail: vanoijen@uow.edu.au; e.m.j.verpoorte@rug.nl; r.c.chiechi@rug.nl

Abstract

This paper describes the fabrication of millimeter-long gold nanowires that bisect the center of microfluidic channels. We fabricated the nanowires by nanoskiving and then suspended them over a trench in a glass structure. The channel was sealed by bonding it to a complementary poly(dimethylsiloxane) structure. The resulting structures place the nanowires in the region of highest flow, as opposed to the walls where it approaches zero, and expose their entire surface area to fluid. We demonstrate active

functionality, by constructing a hot-wire anemometer to measure flow through determining the change in resistance of the nanowire as a function of heat dissipation at low voltage (< 5V). Further, passive functionality is demonstrated by visualizing individual, fluorescently labelled DNA molecules attached to the wires. We measure rates of flow and show that, compared to surface-bound DNA strands, elongation saturates at lower rates of flow and background fluorescence from non-specific binding is reduced.

Keywords: nanoskiving, 3D nanofabrication, nanowires, microfluidics, single-molecule fluorescence imaging

Nanotechnology necessarily involves creating (or co-opting) and manipulating widgets or patterns with dimensions on the nanoscale. Creating nanoscale-widgets can be done by constructing them from smaller components, *e.g.*, synthesizing molecules or growing colloids, or by fabricating them from bulk materials, *e.g.*, lithography. The latter approach falls generally within the purview of nanofabrication, which enables three important advantages of nanotechnology; the ability to interact with micro-scale objects (*e.g.*, cells), the miniaturization of macro-scale functionality (*e.g.*, microelectronics) and access to very high surface-area to volume ratios (*e.g.*, nanowires). Most nanofabrication is confined to a surface, which acts both as a substrate for lithographic processes and an interface between the macroscopic world and the nanoscopic world.

Nanoskiving, a form of edge lithography in which planar structures are sectioned into thin slabs,[1,2] circumvents some of these limitations by forming nanostructures inside a host matrix (usually a cross-linked polymer[3]) that can be manipulated one or several at a time. Compatibility of materials with nanoskiving is defined by mechanical properties,[4] and soft, organic materials that cannot tolerate typical photolithographic processing may be used,[5] such as, for example, molecular and graphene templates to define dimensions with sub-nanometer precision.[6–8] While nanoskiving can be used to fabricate arbitrary shapes,[9–11] it can also be used to form nanowires directly from thin films embedded in polymer matrices[12] and planar crystals.[13,14] The simplest case, sectioning thin metal films, produces metallic

nanowires with control over all three dimensions, that can be millimeters long.[15,16] These wires can be transported, positioned, and aligned directly under a light microscope *via* the (sacrificial) host matrix.[17] This combination of properties is unique to nanoskiving, directly coupling macro and nano regimes and affording access to the entire surface area of the resulting nanowires.

Although nanowires fabricated by nanoskiving are produced serially, this does not have to be a limitation for applications that exploit the functionality of single nanowires, such as microfluidics.[18] Placing nanowires on the floor of a microchannel, however, confines them to a surface and does not take advantage of their discrete nature; there is little functional difference between a thin, photolithographically patterned strip of metal or a nanowire lying flat on a surface. In microfluidic devices viscous forces tend to dominate, leading to laminar flow. The flow profile in this case is zero at the solid/liquid interface and at a maximum in the center of the channel. In sufficiently small channels with large surface-to-volume ratios, this profile is confined such that flow is near-zero over a large portion of the channel. Therefore, experiments or measurements that utilize flow, but involve structures anchored to a surface in the channel for flow interaction in regions which are near or at zero flow, will yield results which are not fully representative of the flow profile. A common example of this problem arises in the *in situ* measurement of rates of flow. Planar lithography confines metallic features to two dimensions and anchors them to a surface, requiring two sensing elements and a heating element to measure flow resistively.[19] Micro-electro-mechanical systems (MEMS) can measure flow mechanically *e.g.*, using external optics,[20] but at the expense of sensitivity and the simplicity of resistive measurements. Another example of an experiment requiring flow in a passive microfluidic system is the study of flow elongation in which long macromolecules (e.g., DNA molecules) are confined to a microfluidic channel and pulled taut by flow for visualization by single-molecule fluorescence.[21–23] If macromolecules are attached to the surface of the bottom of a channel, they are placed in a region of near-zero flow and require high flow rates to achieve elongation. Moreover, non-specific binding of, in particu-

lar, biological molecules to surfaces can significantly lower the recorded signal-to-background ratio of the bound macromolecules of interest. Both of these examples—one active and one passive—would benefit from the (nanoscale) objects of interest being elevated from the surface and held in the center of the channel where the flow is the highest. However, to do so requires the ability to place discrete, three-dimensional nano-objects at arbitrary positions inside of a microchannel, exposing the entire surface-area to the fluid environment.

We bisected microfluidic channels with millimeter-long gold nanowires fabricated by nanoskiving. A schematic of the device architecture is shown in Fig 1. We used glass and PDMS for the rigidity and ease of fabrication, respectively. Holes can be made through the top or bottom layers to access the ends of the nanowires. Because the nanowires extend sufficiently far from the channel, these holes can be drilled or punched by hand and filled with conductive paste to connect the wires to macroscopic leads. The fabrication process is extraordinarily simple due to the discrete nature of nanowires formed by nanoskiving; they are not formed in templates, grown from surfaces, or captured from a liquid suspension. They can be placed one-at-a-time or in arrays as part of a convergent fabrication, *i.e.*, the channels are fabricated independently and therefore can be combined with wires of arbitrary compositions and dimensions without requiring alteration. This simple, convergent fabrication also enables control over the rotation (about the axis normal to the bottom of the channel), height (relative to the bottom of the channel), spacing (of multiple wires), and position (with respect to the inlet and outlet). To demonstrate the utility of integrating discrete nanowires into microfluidic channels, we designed experiments using two device architectures, one active and one passive. The active device demonstrates a two-terminal, hot-wire anemometer that samples flow in the center of the channel in which the entire surface area of the wire is in contact with the fluid being measured. The passive device uses the nanowires as substrates for the attachment of long DNA molecules for the study of elongation.

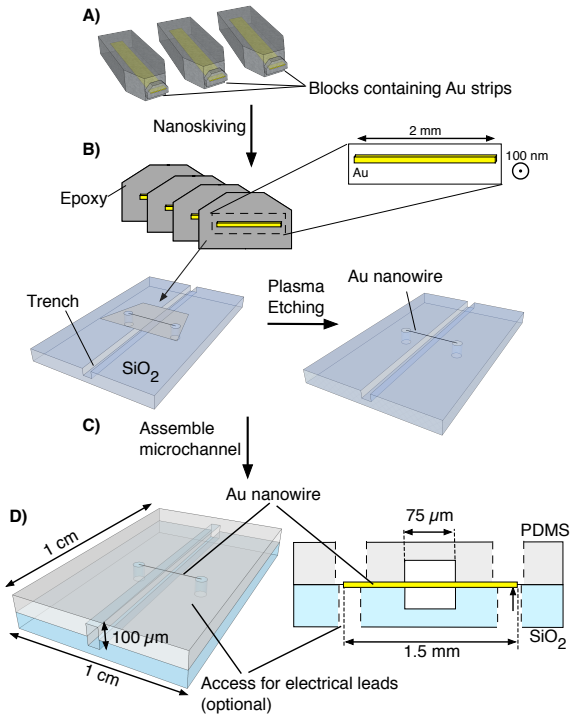

Figure 1: Fabrication scheme and schematics of a microfluidic channel bisected by a gold nanowire. A) Epoxy blocks containing strips of Au are mounted in an ultramicrotome. B) The blocks are sectioned to produce epoxy slabs containing Au nanowires from the cross-section of the Au films. C) The slabs are placed over a pre-etched trench in a glass substrate and the epoxy is removed by plasma etching to leave a free-standing Au nanowire (see Figure 2). D) Left; a schematic of an intact device with access ports for electric leads. Right; a cross-section of the channel showing the positioning of the nanowire.

Results/Discussion

Fabrication

Au nanowires were fabricated by using nanoskiving. A 200-nm or 400-nm-thick gold film was embedded in a block of epoxy from which 200 nm-thick slabs were cut and floated onto a water bath using an ultramicrotome. These slabs containing nanowires were transferred from the water and positioned over 30 μm-deep trenches etched in glass substrates. The epoxy matrix was then removed by etching with O_2 plasma to yield free-standing nanowire(s) spanning the trench in the etched glass. The yield of the wires (when using a well maintained knife) was 100%. The devices were completed by sealing a complementary PDMS channel,

also 30 μm-deep, to the glass to form a closed channel. By stacking Au films, several wires can be installed with arbitrary separation and composition in one channel in a single fabrication step. A detailed description of the entire fabrication procedure is provided in the Supporting Information.

The microfluidic devices were characterized at all stages of fabrication using a combination of optical microscopy, scanning electron microscopy (SEM) and electrical measurement. An image of the finished device is shown in the Supporting Information. To verify that the gold nanowires are suspended freely over the channel, SEM images of the etched glass/nanowire assembly were acquired at a 45° angle (after etching the epoxy). An example of a 200 x 200 nm square nanowire spanning the entire width of a 70 μm-wide trench etched in glass is shown in Figure 2. The wire is completely suspended and does not contact the surface of the glass inside the trench. The angle of the wire with respect to the channel is controlled by rotating the epoxy section containing the wire while the carrier water from the ultramicrotome boat dries. We found it possible, but difficult to achieve perfectly parallel wires, however, the angle had a negligible impact on the subsequent experiments.

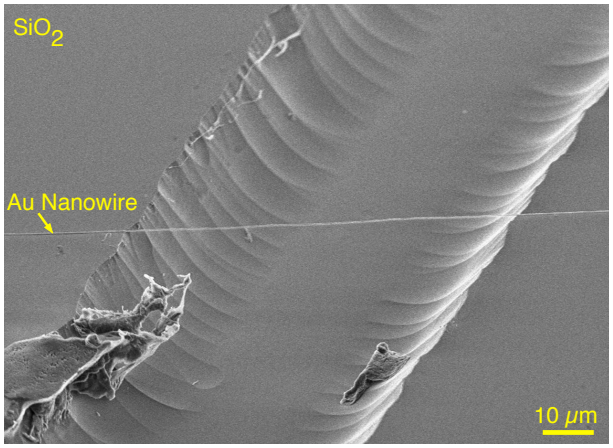

Figure 2: Scanning electron micrograph of 1.5 mm X 200 nm X 200 nm Au nanowire suspended over a 70 μm-wide, 20 μm-deep trench etched into a glass substrate.

Hot-wire Anemometry

Sensors that utilize the principle of heat dissipation can be classified as hot-wire, hot-film, or calorimetric. In microfluidics, the rate of flow can be determined by measuring changes in conductivity affected by changes in temperature as the carrier liquid flows past a metallic conductor. To avoid the risk of physically changing flows in microchannnels by the insertion of relatively bulky structures to measure flow rates, the heating and sensing elements (*e.g.*, "nanowires" in the form of thin strips of metal) are placed at the bottom of the channel where the flow is near zero. This precludes simple hot-wire anemometry and necessitates more complex, multi-wire architectures that include separate heating and sensing elements. Nanowires are small enough that they will not disrupt flow and so can be placed directly in the center of the channel without affecting it. To demonstrate the utility of bisecting microfluidic channels with nanowires fabricated by nanoskiving, we constructed a simple hot-wire anemometer using only a single wire as both the heating and sensing element.

The dimensions of the microfluidic channel test-bed are shown in Figure 1. Ethanol was injected continually into the channel using a syringe pump, and the current response monitored as a function of flow-rate at 0.5, 1.0, 1.5 and 2.0 V (the raw data and a calibration curve are shown in the Supporting Information). Joule heating causes the resistance of the nanowire to increase, which is counteracted by the transport of heat away from the wire by the carrier liquid. Higher rates of flow cool the wire more, and higher voltages give higher sensitivity. Thus, the current at a fixed voltage rises to a plateau as the rate of flow is increased. In order to relate the conductance of the nanowire to flow rates, we replotted these plateaus as relative conductance G/G_0 *versus* pump flow rate, where G is the conductance at a plateau and G_0 is the conductance at zero flow. These data are shown in the left plot of Figure 3 over a range of 0 μL/min to 30 μL/min with increases of 10 μl/min in each step. Data acquired for a nanoskived nanowire placed at the bottom of a channel are shown in red for comparison. These plots clearly show that G/G_0 varies with the rate of flow when the nanowire is freely suspended in the channel, but not when it is placed on

the floor. Increasing the voltage increases the sensitivity (and the magnitude of G/G_0) for the suspended nanowire, but not sufficiently to detect the rate of flow when the nanowire is placed on the bottom of the channel. Ramping the flow rate up and then back down has no effect on the initial value of G/G_0, indicating that there is no hysteresis associated with this approach. Although we only report data up to 30 μL/min, the wires are mechanically stable to sufficiently high rates of flow to rupture the devices; we were unable to break the wires from sheer alone.

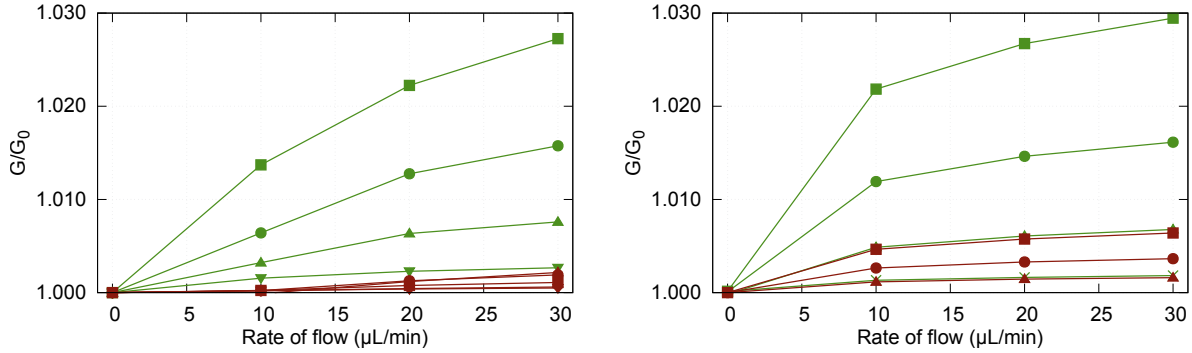

Figure 3: Plots of flow sensor data (left) and simulation (right) from hot-wire anemometers formed by bisecting microfluidic channels with Au wires (green) and placing the wires on the floor of the channel (red). The data show the conductance *versus* rate of flow at 2.0 V (squares), 1.5 V (circles), 1.0 V (triangle), 0.5 V (upside-down triangle) and 0 V (exes).

Simulations

To gain further insight into the effect of the position of the wire on the sensitivity of the hot-wire anemometry we modeled the change in the conductivity of the nanowire numerically using a three-dimensional finite-element simulation (see Supporting Information for details). The right plot of Figure 3 shows simulated data based on the geometry and materials used in the actual device. The simulation agrees qualitatively with the experimental data and is in very close numerical agreement when the wire is bisecting the channel, but over-estimates the response when the wire is placed on the floor of the channel. The probable origin of this discrepancy and the dependence of the sensitivity on the position of the nanowire can be seen in the heatmap plots shown in Figure 4. The temperature distribution in the center of

the microchannel is comparable for both nanowire positions and, as predicted, the bisecting wire is in the region of highest flow while the flow velocity approaches zero at the floor. However, the dominant effect is the proximity of the wire to the glass substrate, which acts as a heat sink, effectively masking the relatively small changes in heat dissipation from the carrier liquid. That is, when the nanowire is suspended freely in the microchannel, the entire surface is in contact with the carrier fluid and therefore heat dissipation is dominated by the fluid. When the wire is placed on the floor, however, one surface is in contact with the relatively enormous mass of the glass substrate, which dominates heat dissipation, *i.e.*, the wire just equilibrates with the glass.

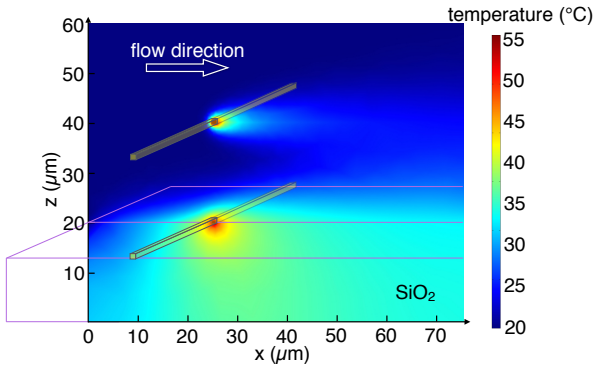

Figure 4: Comparison of the simulated temperature distribution in the center of the microchannel for nanowires positioned at the channel floor and at a height of 20 μm for a rate of flow of 30 μL/min.

The simulation results confirm that the operation of the hot-wire anemometer is contingent upon the entire surface area of the portion of the wire that spans the channel contacting the carrier fluid. Thus, this method of flow-sensing is nanoscopic in origin and relies on the ability of nanoskiving to produce discrete, three-dimensional nanowires that can be positioned arbitrarily. It is also simple, requiring only the ability to apply voltage and measure current. For potential applications beyond this proof-of-concept, the choice of nanowire dimensions and composition is limited only by the loose constraints of nanoskiving.

Suspended DNA curtains

The observation of protein-DNA interactions at the single-molecule level represents a powerful approach to understand the molecular mechanisms that are responsible for the copying, reading, and repairing of the genetic information stored in DNA.[21–23] A frequently used method relies on the fluorescence imaging of long, stretched DNA molecules and the proteins interacting with it. A common requirement for such techniques is the coupling of one end of a long, linear DNA molecule to a planar surface[24] and its stretching by a laminar flow.[25,26] However, a major drawback of this approach is that the DNA molecule and proteins bound to it are susceptible to non-specific interactions with the surface.[22,24,27–29] Further, stretching surface-tethered DNA molecules by flow is challenging because of the low rate of flow close to the surface in a laminar, Poiseuillian flow. By binding DNA molecules to a gold nanowire bisecting a flow cell (microfluidic channel), we anchor DNA molecules far away from the four walls of the channel, thereby preventing any interaction of the DNA with the surface. Furthermore, being attached to an elevated nanowire, the DNA molecules experience a more uniform flow and higher rate of flow than if they were tethered to a surface, allowing a lower overall rate of flow.

The attachment of many linear DNA molecules to a suspended nanowire results in a pattern that is defined as a "DNA curtain."[30] A curtain of DNA molecules grants the possibility of recording several single-molecule events at the same time and allows the study of DNA-protein interactions at high local DNA concentration. These curtains are usually formed by planar lithography, using e-beam writing and etching to define barriers that interrupt a passivating lipid layer. Defining this passivating layer is a critical step in the formation of the curtains and for imaging the DNA. Bisecting microfluidic channels simplifies the formation of curtains by eliminating the planar lithography steps and obviating the need for passivation of a surface. In principle, these advantages come without any significant loss in the quality of the recorded images as compared to fluorescence imaging approaches visualizing proteins interacting with long DNA molecules.

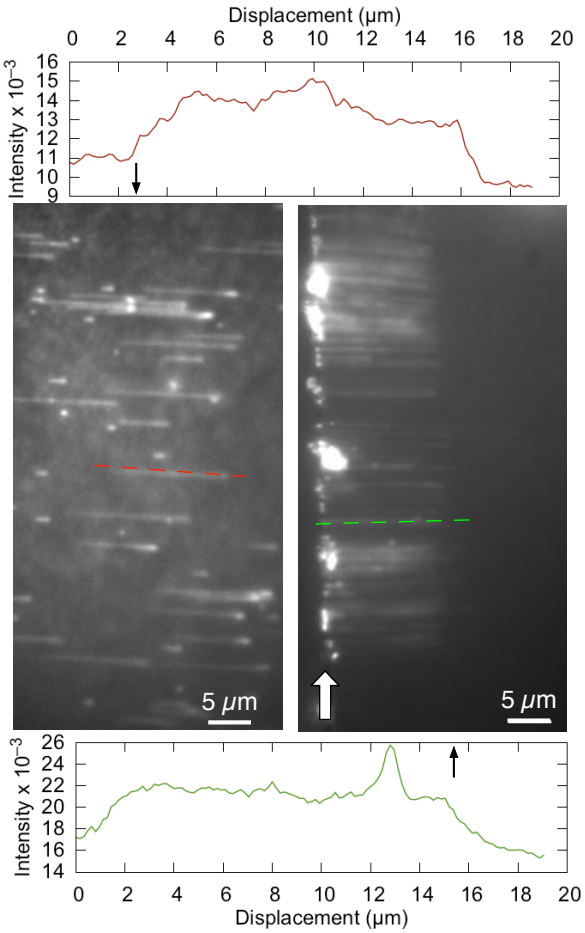

Figure 5: Averaged fluorescence images of immobilized DNA elongated by flow. Intercalating dye (SYTOX Orange) was present in solution to specifically stain and visualize double-stranded DNA. Left; a typical experiment in which the DNA is bound to random positions on the bottom surface of a microfluidic channel. Right; a typical experiment in which the DNA is bound to a Au nanowire bisecting the microfluidic channel at the midpoint. The position of the nanowire is indicated with a white arrow. A curtain of DNA extends outward from the wire in the direction of flow (from left to right). Intensity profiles corresponding to the green and red dashed lines are shown above and below the images; the x-axis is the displacement along the dashed lines. In the surface-bound experiment (left, top) there is significant background from non-specific binding and lower signal intensity. In the nanowire-bound experiment (right, bottom) there is no non-specific binding, leading to a significantly reduced level of background and a higher signal intensity.

Using a similar channel geometry as shown in Figure 1, we coupled DNA molecules to the suspended nanowires using standard Au-S chemistry to attach biotin/streptavidin followed by the introduction of biotinylated DNA. By specifically coupling one end of linear lambda-phage DNA (48.5 kilobases of double-stranded DNA; contour length 16.3 μm) to the

nanowire, we obtained a curtain of DNA molecules that can be stretched by flow. Stable attachment at only the biotinylated end of the DNA was confirmed by reversing the flow direction. The DNA density on the nanowire was controlled by varying the DNA concentration and the time of incubation. At sufficiently low densities, single molecules could easily be resolved. Figure 5 shows a DNA curtain attached to a nanowire (in the presence of intercalating dye to stain the double-stranded DNA fluorescently) alongside an image of surface-bound DNA molecules. Other than the obvious difference between DNA molecules arranged along a nanowire and molecules randomly-bound to a surface, the experiment using the nanowire results in less image artifacts due to non-specific binding (visible as diffuse shapes between isolated DNA molecules in the left image). Intensity profiles along the lengths of DNA molecules (Figure 5 top and bottom) show that the signal intensity is indeed slightly higher and more uniform in the curtain than in the randomly-bound surface case. We ascribe this difference to the complete lack of background signal from the separation of the curtain from the floor of the channel; *i.e.*, non-specific binding still occurs, but it is far removed from the focal plane.

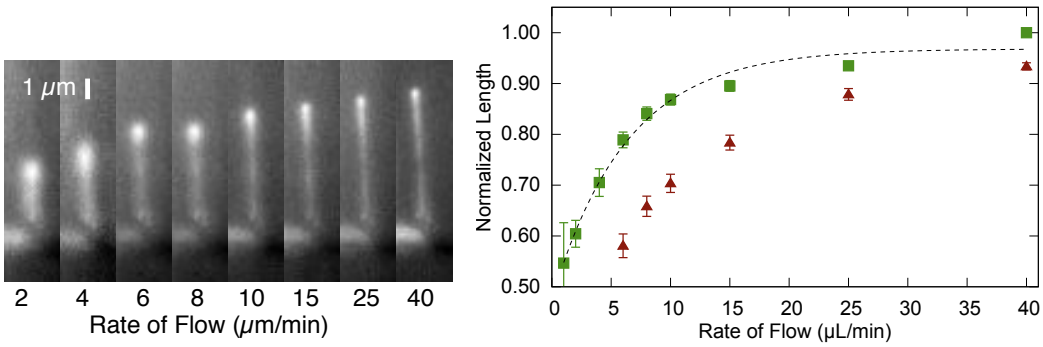

Figure 6: Left; sequential images of the elongation of lambda-phage DNA bound to a Au nanowire bisecting the microfluidic channel at the midpoint. Right; extension-force curve of lambda-phage DNA showing the normalized length averaged from six DNA molecules bound to nanowires (green squares) and from twelve DNA molecules bound to the surface of the same device (red triangles) *versus* rate of flow. It shows the influence of the different flow velocities at the nanowire and the surface. The dashed lines are exponential fit to guide the eye.

The ability to image individual, nanowire-coupled and flow-stretched DNA molecules

at high signal-to-background ratios allowed the determination of the length of the DNA molecule as a function of rate of flow, ranging between 1 and 40 μl/min (measured at the pump). These flow-extension data are shown in Figure 6. At low rates of flow, large DNA fluctuations orthogonal to the flow direction were visible and the total DNA extension was measured to be significantly less than the contour length. This behavior represents the entropic collapse of the long DNA molecule at low stretching forces.[31] At high rate of flow, such fluctuations were no longer visible and the hydrodynamic force increased the mean extension of the DNA molecules. The relation between a force applied to the DNA and its extension has been extensively studied and well described by the Worm-Like Chain (WLC) model.[31–34] In our setup, the tension along the DNA molecule decreases as one moves from the tethered end to the free end, instead of being uniformly applied to the end as assumed in the WLC model. However, even in this case the length will asymptotically approach the contour length (0.34 nm per basepair).[24] The lengths of six DNA molecules at various rates of flow were measured, and their average length was normalized by their average length at 40 μl/min (Figure 6). At relatively low rates of flow, 5 μl/min, the DNA reaches 75% of its contour length. By contrast, DNA bound to the floor of the same microchannel did not reach 75% extension until 15 μl/min. The origin of this difference is the higher rate of flow experienced by the nanowire-bound DNA, demonstrating that the presence of the nanowire does not interfere significantly with laminar flow in the center of the channel. Although we do not have experimental evidence that the wires have no effect on laminar flow at all, this observation is important, as the apparent non-interference with the laminar flow is a crucial prerequisite for the further application of these nanowires to flow-based measurements.

Conclusions

Applications of microfluidic devices that take advantage of flow, but that are constrained to the solid-liquid interface at the walls of the channel, require high rates of flow and must compete with non-specific binding. Measurements of flow upstream or downstream of an experiment are often limited to sampling the rate of flow at the walls, where it is lowest. Bisecting a microfluidic channel with a gold nanowire allows experiments to be performed in the center of the channel, where the rate of flow is the highest. Measurements of flow can then be conducted at the region of the highest rate of flow and directly at a point of interest. However, forming the discrete, millimeter-long gold nanowires necessary to bisect microfluidic channels is prohibitively complex using standard lithographic techniques. Nanoskiving enables the fabrication of these ultra-long nanowires and facilitates the implementation of the wires, which are simply scooped off of the surface of a water bath directly onto a channel as they are formed. While it is possible to place very thin (micron-sized) wires in a microfluidic channel, true nano-scale wires benefit from a very large surface-to-volume ratio, low drag, and minimized effects on laminar flow.

Methods of flow-sensing based on heat-dissipation rely on a heating element and a downstream sensor to achieve a temperature gradient sufficient to measure a change in conductivity. However, a single nanowire is sensitive enough to serve both as the heating and sensing element if it is suspended in a microfluidic channel. Finite-element analysis reveals that this sensitivity arises from having the entire surface area of the wire in contact with the carrier liquid, eliminating the mass of the substrate as a heat sink. Binding DNA molecules to nanowires similarly exposes the entire surface of the nanowire-DNA assembly to the carrier fluid, eliminating background signal from non-specific binding in fluorescence experiments and forming a curtain of DNA along the length of the nanowire. Flow-elongation measurements reveal that the DNA reaches maximum extension at lower rates of flow (measured at the pump) because the rate of flow within the channel is highest away from the walls of the channel.

This fabrication technique provides the ability to place a nanoscale object directly in the center of a microfluidic channel, gaining access to the peak rate of flow. We demonstrate the technique with gold nanowires, but Nanoskiving is compatible with virtually any non-brittle material. Any experiment or measurement that utilizes flow across a stationary widget can therefore potentially benefit from this technique.

Methods/Experimental

Au nanowires were fabricated by nanoskiving. First, 200 nm or 400 nm thick gold films were deposited onto a silicon wafer (used as-received) through a Teflon mask by thermal evaporation. The gold films were then covered with a layer of Epofix epoxy (Catalog #1232, Electron Microscope Sciences) and, after curing, the epoxy was separated from the wafer mechanically. The gold films remained attached to the epoxy. The epoxy was rough cut with a jeweler's saw into small enough pieces to fit into a "coffin mold" used to form standard blocks for ultramicrotomy. The mold was filled with more epoxy and then cured at 60 °C overnight. The result was a 200 nm or 400 nm thick gold film embedded in a block of epoxy. 200 nm thick slabs were sectioned and floated onto a water bath using an ultramicrotome (Leica UC-6). These slabs, containing nanowires, were transferred from the water onto the appropriate substrate (*e.g.*, etched glass). Nanowires were liberated from the epoxy matrix by O_2 plasma dry etching for 1 hour at 100 mTorr, 30 W, using a Harrick Plasma Cleaner.

For the glass substrates, a prefabricated 4" square borofloat wafer coated with chromium and photoresist (Telic, USA, MED027021P) was exposed to a UV light source through a semitransparent mask. Developer (AZ 351 B Developer, AZ Electronic Materials, Germany) was used to remove the exposed photoresist. Chrome etch (Chrome Etch 18, OSC-OrganoSpezialChemie, Germany) was used to remove the chrome layer beneath. The exposed glass was etched using HF. After etching the unexposed photoresist and chrome were removed using acetone and chrome etch.

Soft lithography was preformed using a 40 μm-high SU-8 master fabricated on a glass borofloat wafer (10 cm diameter, 0.7 mm thick). The wafer was cleaned following standard wet cleaning protocols and dried on a hot plate. A spin coater was used to coat the wafer with a 40 μm-thick layer of SU-8 50 (Microchem). After a baking step to evaporate the solvent in the SU-8, the wafer was exposed to UV light through a semi-transparent mask. After exposure a baking step was preformed to cross-link the exposed SU-8. Developer (md-Dev 600, Micro Resist Technology, Germany) was used to remove the unexposed SU-8. PDMS monomer (Sylgard 184, Dow Corning) was mixed with PDMS curing agent in a 10:1 (w/w) ratio and the mixture was placed under a vacuum for 30 minutes to remove any bubbles. The uncured PDMS was poured over the wafer and cured on a hot-plate for 3 hours at 60 °C. After curing, the desired patterns were cut from the PDMS slab using a sharp razor blade. To create fluid inlets and outlets, a biopsy puncher with a diameter of 1.2 mm was used.

For flow-sensing measurements the nanowire was connected with a Keithley 2400 SourceMeter. The I-V plots of the nanowire suspended in microfluidic channel before and after the injection of the ethanol were recorded before the flow measurements. The current through the nanowire at different voltages was recorded with step size of 0.1 V. After that, a series of voltages (0.5V, 1.0V, 1.5V, 2V) was applied to the nanowire and the resulting current was measured over time at different rates of fluid flow. The fluid inlet of the nanowire device was connected to a 10 ml syringe (Terumo Syringe) with a diameter of 15.8 mm, and the fluid outlet was coupled to a waste beaker. Polyethylene tubing (PE60, 0.76 mm inner diameter, 1.22 mm outer diameter, Bioseb) was used to make the fluid connections. The inlet rates of the flow were set manually by a syringe pump (Spritzenpumpe LA-100, Landgraf Laborsysteme HLL GmbH). The used fluid was ethanol.

We used a finite-element simulation (COMSOL Multiphysics) to model a simplified three dimensional geometry of a microchannel with a 75 μm (width) by 60 μm (height) rectangular cross section and a length of 70 μm. A nanowire with a quadratic cross section of 200 nm by 200 nm bisects the microchannel at 20 μm channel height 25 μm downstream of the inlet, or

is positioned at the floor of the microchannel, respectively. (See Figure 4 in the Main Text.)

The stationary flow profile in the channel was calculated by evaluating the Stokes equation for an incompressible fluid (using the viscosity and density of ethanol). No-slip conditions were chosen for all boundaries except for an outlet (0 Pa exit pressure) and an inlet with a laminar inflow rate ranging from 0 to 30 μL/min (at a constant inflow temperature of 293 K). The electrical current through the nanowire was modeled by using the boundary conditions of a potential difference applied at both ends of the nanowire (electrical conductivity of gold) separated by 75 μm. In the experiment, the nanowire extends beyond the width of the microchannel and, thus, the potential difference is applied effectively over a wire length of several hundred micrometers. In the simulation, identical potential drops *per wire length* were used. For better comparability, in Figure 3 (right) in the Main Text, the simulated potentials are stated as values corresponding to the equivalent longer *experimental* wire lengths.

To simulate heat transfer caused by the electrical current, the nanowire was coupled to the surrounding liquid by employing a heat equation for convective and conductive heating. As boundary conditions, thermal isolation was chosen for the side walls and ceiling of the microchannel; heat dissipation at the microchannel floor was modeled by a borosilicate block of 20 μm height underneath.

Flow cells were constructed to allow the incorporation of a suspended nanowire. Glass coverslips (Marienfeld-Superior) were cleaned by successive sonication in 2% (v/v) Hellmanex III (Hellma Analytics), in 100% ethanol (Avantor), and in 1 M KOH (Sigma-Aldrich). After each step, the slides were rinsed thoroughly with milli-Q water. The coverslips were 60 mm long, 24 mm wide, and 0.13-0.16 mm thick. On each slide, two strips of 50 μm thick double-sided tape (3M) were deposited so that a 40 x 4 mm sized channel was obtained. A 0.7 mm thick, 5 x 45 mm sized borofloat glass (TELIC) was used as flow chamber top. A 60 μm wide and 20 μm deep channel was excavated in this slide by HF etching (see above). Two holes 40 mm apart were made in the channel for the inlet and outlet tubing.

Subsequently, an array of gold nanowires was deposited across the channel. The gold nanowires had a diameter of 400 nm and a length of 1.5 mm. With the nanowires on the bottom face, the etched slide was positioned on the two tape strips while taking care that the etched channel was centered. The assembled flow cell was sealed with epoxy (Bison). Two homemade ports (3d printed in ABS) were glued with epoxy on top of the inlet/outlet holes. They were used as support for the polyethylene tubing (PE60, 0.76 mm inner diameter, 1.22 mm outer diameter, Bioseb). After placing the flow cell on the microscope sample stage, the outlet tube was connected to a syringe pump (New Era Pump Systems Inc.) used to control the flow of buffer.

The gold nanowires were modified with DNA molecules tethered through Au-S bond and biotin-streptavidin-biotin linkages. First, the suspended gold nanowires in the flow cell were incubated with 10 mM cysteamine (cysteamine hydrochloride from Sigma-Aldrich) in ethanol for at least two hours, functionalizing the surface with primary amines *via* the formation of a self-assembled monolayer. After washing the ethanol solution out, the modified gold nanowires were incubated with 0.3 mg/ml NHS-biotin (Thermo Scientific) in PBS (pH=8.2) for 1 hour to functionalize them with surface-bound biotin. Subsequently, they were incubated with 0.2 mg/ml streptavidin (Sigma-Aldrich) in PBS (pH=8.2) for 30 minutes to bind the biotin resulting in nanowires modified with surface-bound streptavidin. Finally, forked lambda-phage DNA molecules, biotinylated at the 5' end of the fork (3), were flowed into the chamber in 20 mM Tris (pH=7.5), 2 mM EDTA, 50 mM NaCl, 1 mg/ml bovine serum albumin (BSA), and 0.025% Tween20. Excess DNA was removed by washing with the same buffer. 100 nM SYTOX Orange (Invitrogen) was used to stain the DNA molecules. The Sytox-stained DNA molecules were excited with a 532 nm solid-state laser (Coherent Sapphire 532-200 CW) at 25 Wcm^{-2} in epifluorescence mode. The resulting fluorescent signal was collected through a 100x oil-immersion TIRF objective (Olympus, 1.49 NA) and recorded on an EM-CCD camera (Hamamatsu).

Associated Content

Supporting Information is available free of charge on the ACS Publications Website. Device assembly and additional data, micrographs and photographs of flow-sensing and DNA stretching experiments.

Acknowledgment

This work was supported by an ERC Starting Grant (281098; SINGLEREPLISOME) and an NWO Vici grant (680-47-607) to AvO. RCC and YZ acknowledge ERC Starting Grant (335473; MOLECSYNCON). PEO and EV acknowledge funding provided by EU Program HEALTH.2012.1.4-2 [Medical technology for transplantation and bioartificial organs], GA:304842. We thank Dr.Marc Stuart for gold sputtering and Jasper van den Berg for assistance with the SEM measurements.

References

1. Xu, Q.; Rioux, R. M.; Dickey, M. D.; Whitesides, G. M. Nanoskiving: A New Method to Produce Arrays of Nanostructures. *Acc. Chem. Res.* **2008**, *41*, 1566–1577.

2. Lipomi, D. J.; Martinez, R. V.; Whitesides, G. M. Use of Thin Sectioning (Nanoskiving) to Fabricate Nanostructures for Electronic and Optical Applications. *Angew. Chem. Int. Ed.* **2011**, *50*, 8566–8583.

3. Mays, R. L.; Pourhossein, P.; Savithri, D.; Genzer, J.; Chiechi, R. C.; Dickey, M. D. Thiol-Containing Polymeric Embedding Materials for Nanoskiving. *J. Mater. Chem. C* **2013**, *1*, 121–130.

4. Lipomi, D. J.; Martinez, R. V.; Rioux, R. M.; Cademartiri, L.; Reus, W. F.; Whitesides, G. M. Survey of Materials for Nanoskiving and Influence of the Cutting Process on the Nanostructures Produced. *ACS Appl. Mat. Interf.* **2010**, *2*, 2503–2514.

5. Lipomi, D. J.; Chiechi, R. C.; Dickey, M. D.; Whitesides, G. M. Fabrication of Conjugated Polymer Nanowires by Edge Lithography. *Nano Let.* **2008**, *8*, 2100–2105.

6. Zaretski, A. V.; Marin, B. C.; Moetazedi, H.; Dill, T. J.; Jibril, L.; Kong, C.; Tao, A. R.; Lipomi, D. J. Using the Thickness of Graphene to Template Lateral Subnanometer Gaps between Gold Nanostructures. *Nano Letters* **2015**, *15*, 150105140507005–640.

7. Pourhossein, P.; Chiechi, R. C. Fabricating Nanogaps by Nanoskiving. *J. Vis. Exp.* **2013**, *75*, e50406–e50406.

8. Pourhossein, P.; Chiechi, R. C. Directly Addressable Sub-3 nm Gold Nanogaps Fabricated by Nanoskiving Using Self-Assembled Monolayers as Templates. *ACS Nano* **2012**, *6*, 5566–5573.

9. Xu, Q.; Perez-Castillejos, R.; Li, Z.; Whitesides, G. M. Fabrication of High-Aspect-Ratio Metallic Nanostructures Using Nanoskiving. *Nano Let.* **2006**, *6*, 2163–2165.

10. Xu, Q.; Rioux, R. M.; Whitesides, G. M. Fabrication of Complex Metallic Nanostructures by Nanoskiving. *ACS Nano* **2007**, *1*, 215–227.

11. Lipomi, D. J.; Kats, M. A.; Kim, P.; Kang, S. H.; Aizenberg, J.; Capasso, F.; Whitesides, G. M. Fabrication and Replication of Arrays of Single- or Multicomponent Nanostructures by Replica Molding and Mechanical Sectioning. *ACS Nano* **2010**, *4*, 4017–4026.

12. Wiley, B.; Lipomi, D.; Bao, J.; Capasso, F.; Whitesides, G. Fabrication of Surface Plasmon Resonators by Nanoskiving Single-Crystalline Gold Microplates. *Nano Let.* **2008**, *8*, 3023–3028.

13. Lipomi, D. J.; Chiechi, R. C.; Reus, W. F.; Whitesides, G. M. Laterally Ordered Bulk Heterojunction of Conjugated Polymers: Nanoskiving a Jelly Roll. *Adv. Func. Mater.* **2008**, *18*, 3469–3477.

14. Wan, A.; Wang, T.; Yin, T.; Li, A.; Hu, H.; Li, S.; Shen, Z. X.; Nijhuis, C. A. Plasmon-Modulated Photoluminescence of Single Gold Nanobeams. *ACS Photonics* **2015**, *2*, 1348–1354.

15. Qiaobing Xu,; Gates, B. D.; ; Whitesides, G. M. Fabrication of Metal Structures with Nanometer-Scale Lateral Dimensions by Sectioning Using a Microtome. *J. Am. Chem. Soc.* **2004**, *126*, 1332–1333.

16. Xu, Q.; Bao, J.; Capasso, F.; Whitesides, G. M. Surface Plasmon Resonances of Free-Standing Gold Nanowires Fabricated by Nanoskiving. *Angew. Chem.* **2006**, *118*, 3713–3717.

17. Lipomi, D. J.; Ilievski, F.; Wiley, B. J.; Deotare, P. B.; Lončar, M.; Whitesides, G. M. Integrated Fabrication and Magnetic Positioning of Metallic and Polymeric Nanowires Embedded in Thin Epoxy Slabs. *ACS Nano* **2009**, *3*, 3315–3325.

18. Dawson, K.; Strutwolf, J.; Rodgers, K. P.; Herzog, G.; Arrigan, D. W. M.; Quinn, A. J.; O'Riordan, A. Single Nanoskived Nanowires for Electrochemical Applications. *Anal. Chem.* **2011**, *83*, 5535–5540.

19. Schöler, L.; Lange, B.; Seibel, K.; Schäfer, H.; Walder, M.; Friedrich, N.; Ehrhardt, D.; Schönfeld, F.; Zech, G.; Böhm, M. Monolithically Integrated Micro Flow Sensor for Lab-On-Chip Applications. *Microelectronic Engineering* **2005**, *78-79*, 164–170.

20. Cheri, M. S.; Latifi, H.; Sadeghi, J.; Moghaddam, M. S.; Shahraki, H.; Hajghassem, H. Real-Time Measurement of Flow Rate in Microfluidic Devices Using a Cantilever-Based Optofluidic Sensor. *Analyst* **2013**, *139*, 431–438.

21. Dulin, D.; Lipfert, J.; Moolman, M. C.; Dekker, N. H. Studying Genomic Processes at the Single-Molecule Level: Introducing the Tools and Applications. *Nat Rev Genet* **2013**, *14*, 9–22.

22. Hua, B.; Han, K. Y.; Zhou, R.; Kim, H.; Shi, X.; Abeysirigunawardena, S. C.; Jain, A.; Singh, D.; Aggarwal, V.; Woodson, S. A.; Ha, T. An Improved Surface Passivation Method for Single-Molecule Studies. *Nat Meth* **2014**, *11*, 1233–1236.

23. Robinson, A.; van Oijen, A. M. Bacterial Replication, Transcription and Translation: Mechanistic Insights from Single-Molecule Biochemical Studies. *Nat Rev Micro* **2013**, *11*, 303–315.

24. Granéli, A.; Yeykal, C. C.; Prasad, T. K.; Greene, E. C. Organized Arrays of Individual DNA Molecules Tethered to Supported Lipid Bilayers. *Langmuir* **2006**, *22*, 292–299.

25. Tanner, N. A.; Loparo, J. J.; Hamdan, S. M.; Jergic, S.; Dixon, N. E.; van Oijen, A. M. Real-Time Single-Molecule Observation of Rolling-Circle DNA Replication. *Nucleic Acids Research* **2009**, *37*, e27–e27.

26. Tanner, N. A.; van Oijen, A. M. In *Single Molecule Tools, Part B:Super-Resolution, Particle Tracking, Multiparameter, and Force Based Methods*; in Enzymology, N. G. W. B. T. M., Ed.; Academic Press, 2010; Vol. Volume 475; pp 259–278.

27. Fazio, T.; Visnapuu, M.-L.; Wind, S.; Greene, E. C. DNA Curtains and Nanoscale Curtain Rods: High-Throughput Tools for Single Molecule Imaging. *Langmuir* **2008**, *24*, 10524–10531.

28. Ha, T.; Rasnik, I.; Cheng, W.; Babcock, H. P.; Gauss, G. H.; Lohman, T. M.; Chu, S. Initiation and Re-Initiation of DNA Unwinding by the Escherichia coli Rep Helicase. *Nature* **2002**, *419*, 638–641.

29. Rasnik, I.; Myong, S.; Cheng, W.; Lohman, T. M.; Ha, T. DNA-Binding Orientation and Domain Conformation of the E. coli Rep Helicase Monomer Bound to a Partial Duplex Junction: Single-molecule Studies of Fluorescently Labeled Enzymes. *J. Mol. Bio.* **2004**, *336*, 395–408.

30. Collins, B. E.; Ye, L. F.; Duzdevich, D.; Greene, E. C. In *Quantitative Imaging in Cell Biology*; Biology, J. C. W., in Cell, T. W. B. T. M., Eds.; Academic Press, 2014; Vol. Volume 123; pp 217–234.

31. Bustamante, C.; Smith, S. B.; Liphardt, J.; Smith, D. Single-Molecule Studies of DNA Mechanics. *Cur. Op. Struct. Bio.* **2000**, *10*, 279–285.

32. Baumann, C. G.; Smith, S. B.; Bloomfield, V. A.; Bustamante, C. Ionic effects on the elasticity of single DNAmolecules. *Proc. Natl. Acad. Sci. USA* **1997**, *94*, 6185–6190.

33. Bustamante, C.; Marko, J. F.; Siggia, E. D.; Smith, S. Entropic Elasticity of Lambda-Phage DNA. *Science* **1994**, *265*, 1599–1600.

34. Marko, J. F.; Siggia, E. D. Stretching DNA. *Macromolecules* **1995**, *28*, 8759–8770.

Graphical TOC Entry

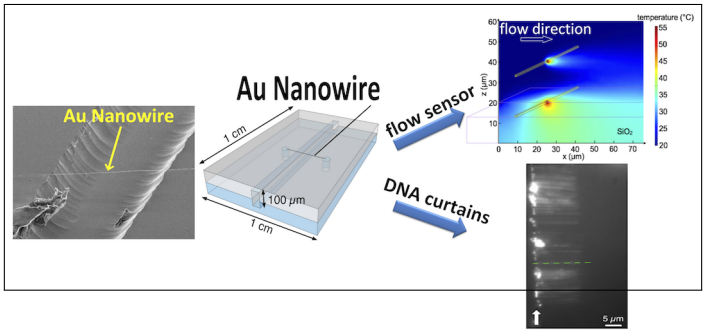

A gold nanowire fabricated by nanoskiving is placed over a trench etched in glass and fused with a complementary elastomeric slab to form a microfluidic channel bisected by a nanowire that acts as a flow-sensor and a scaffold for imaging curtains of DNA.